The origin of anomalous diffusion and non-Gaussian effects for hard spheres: analysis of three-time correlations

1999 J. Phys.: Condens. Matter 11 A277

(http://iopscience.iop.org/0953-8984/11/10A/025)

J. Phys.: Condens. Matter **11** (1999) A277–A283. Printed in the UK PII: S0953-8984(99)00066-1

The origin of anomalous diffusion and non-Gaussian effects for hard spheres: analysis of three-time correlations

B Doliwa and A Heuer

Max-Planck-Institut für Polymerforschung, Postfach 3148, D-55021 Mainz, Germany

Received 2 October 1998

Abstract. We present new simulation results on a hard-sphere system at high densities. Using three-time correlations, we can account for the anomalous diffusion, which results from a homogeneous back-dragging effect. Furthermore, we calculate the non-Gaussian parameter and connect it to the existence of dynamic heterogeneities.

1. Introduction

In recent years the nature of the non-exponential relaxation of glass-forming liquids close to T_g has been elucidated by a variety of experimental techniques; see [Edi96] and [Böh98] for an overview. One way of getting additional information is to analyse three-time correlation functions in addition to the standard two-time correlation functions, as realized in multidimensional NMR experiments. On this basis it is possible to decide whether the non-exponentiality is mainly due to a homogeneous scenario (intrinsic non-exponentiality related to systematic back-and-forth dynamics) or a heterogeneous scenario (superposition of different exponential processes). In a previous publication [Dol98] these concepts have been applied to computer simulations of a hard-sphere system which is well represented experimentally by colloidal suspensions [Meg91]. We observed that the dynamics at short times (the β-regime) is dominated by the presence of a cage formed by surrounding particles. This results in a systematic back-dragging effect, corresponding to a mainly homogeneous scenario. In the α-regime most particles have escaped their initial cages. Then they encounter fast or slow regions in the liquid, arising, e.g., from inhomogeneities in density. The simplest model for this situation would be an ensemble of independently diffusing particles with different mobilities.

The goal of the present work is to quantify the hard-sphere dynamics in terms of homogeneous and heterogeneous contributions for all timescales. In an extension of our previous work, we introduce appropriate measures for homogeneous and heterogeneous contributions. They help to elucidate the physics of the sublinear diffusion in the β-regime and the non-Gaussian parameter.

2. Simulation details

We perform conventional Monte Carlo dynamics with periodic boundary conditions on a system of a thousand hard spheres with a size polydispersity of 10%. The algorithm is described in [Cic90, Dol98]. For the β- and α-regimes, the mean step size has been chosen to give an

0953-8984/99/SA0277+07$19.50

acceptance rate of 50% for each move. We checked that, apart from an overall scaling, the dynamics is not influenced by changing the mean step size for these time regions.

At very short times, we perform separate simulation runs with a reduced step size, in order to obtain the microscopic dynamics. This is necessary, because we want to define a density-independent timescale by fixing the short-time diffusion constant, i.e. $\langle r^2(t)\rangle = 6D_0t$, where t is very small. We use $D_0 \equiv \frac{1}{160}$ and set the unit of length equal to the mean particle diameter, as was done by Fuchs *et al* [Fuc98].

The highest density analysed in this paper is $\phi \equiv \langle \frac{4}{3}\pi R_i^3\rangle N/V = 0.58$. At this high packing fraction, we have chosen a very long equilibration time (5×10^7 MCS) to avoid aging effects occurring during the measurement. Interestingly, the non-Gaussian parameter (NGP) turns out to be a very sensitive indicator for the degree of equilibration.

In figure 1 we plot the incoherent scattering function $F_2(t) = \langle \cos \vec{q}(\vec{r}(t) - \vec{r}(0))\rangle$ for $q = 2\pi$ and the mean square displacement, clarifying the timescales of our simulations.

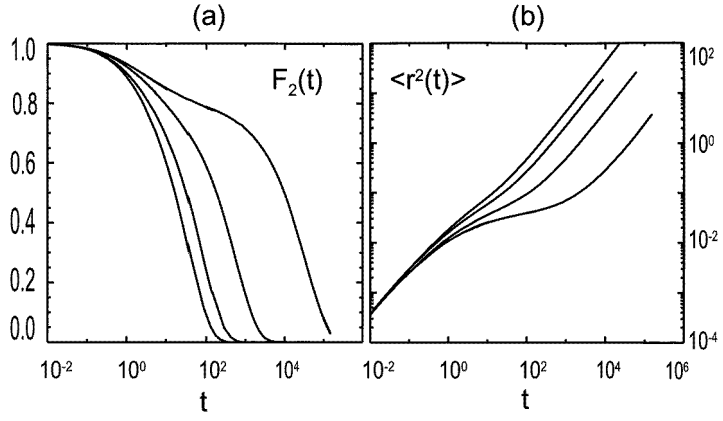

Figure 1. (a) The two-time correlation function $F_2(t) = \langle \cos \vec{q}(\vec{r}(t) - \vec{r}(0))\rangle$ for $q = 2\pi$ which is close to the maximum of the structure factor. The curves are plotted for the densities $\phi = 50, 53, 56$ and 58%, from left to right. (b) The mean square displacements $\langle r^2(t)\rangle$ for the densities in (a), again from left to right.

3. Three-time correlations: the homogeneous part

As shown in our recent work [Dol98], we can gain new insight into the dynamics by analysing three-time correlation functions. For a given time t we define the conditional probabilities $p_\parallel(\vec{r}_{12} \cdot \widehat{r}_{01}|r_{01}; t)$, $p_\perp(\vec{r}_{12} \cdot \widehat{u}_{01}|r_{01}; t)$ and $p_{zz}(z_{12}|z_{01}; t)$ with $\vec{r}_{mn} \equiv \vec{r}(nt) - \vec{r}(mt)$, $r_{mn} \equiv |\vec{r}_{mn}|$. Here $\widehat{u}_{01}$ is an arbitrary vector perpendicular to $\vec{r}_{01}$, the hat denoting a unit vector. We introduce the abbreviations $x_{12} \equiv \vec{r}_{12} \cdot \widehat{r}_{01}$ and $y_{12} \equiv \vec{r}_{12} \cdot \widehat{u}_{01}$ for later purposes. Thus, $p_\parallel(x_{12}|r_{01}; t)$ denotes the probability that a particle moves during the second time interval the distance x_{12}, projected onto the vector $\widehat{r}_{01}$, under the condition that it covered a distance r_{01} in the first time interval. The probability function $p_\perp(y_{12}|r_{01}; t)$ is defined analogously, yielding information about the distance y_{12} travelled perpendicular to the first step. Finally, $p_{zz}(z_{12}|z_{01}; t)$ includes the information about the projection of both steps onto a randomly chosen direction.

For non-exponential relaxation, as displayed by supercooled liquids, memory effects are present, resulting in a strong dependence of p_{zz} and $p_{\parallel,\perp}$ on z_{01} and r_{01}, respectively. We see the typical situation in figure 2, where all of these probability distributions are shown for a

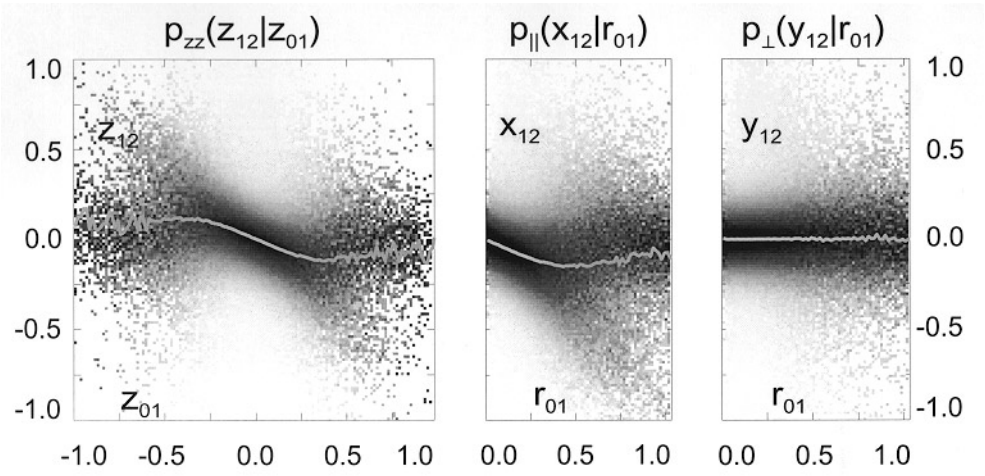

Figure 2. The conditional probabilities $p_{zz}(z_{12}|z_{01};t)$, $p_{\parallel}(x_{12}|r_{01};t)$ and $p_{\perp}(y_{12}|r_{01};t)$ for a time $t \approx 400$ in the β-regime, where $x_{12} \equiv \vec{r}_{12} \cdot \widehat{r}_{01}$ and $y_{12} \equiv \vec{r}_{12} \cdot \widehat{u}_{01}$. z_{01} and z_{12} denote the projections of the subsequent displacements onto an arbitrary direction. The dark areas correspond to high probabilities. The average values $c_{zz}(z_{01})$, $c_{\parallel}(r_{01})$ and $c_{\perp}(r_{01})$ are indicated by the light traces. Note that the unit of length is greater than that used in [Dol98] by a factor of 2.

density of $\phi = 58\%$ at a time $t \approx 400$ in the β-region. The main features of these plots are the non-zero displacements, $c_{zz}(z_{01}) \equiv \langle z_{12} \rangle$, $c_{\parallel}(r_{01}) \equiv \langle x_{12} \rangle$ and $c_{\perp}(r_{01}) \equiv \langle y_{12} \rangle$ as indicated, and the widths $\sigma_{zz}(z_{01})$, $\sigma_{\parallel}(r_{01})$ and $\sigma_{\perp}(r_{01})$, where, e.g.,

$$\sigma_{\parallel}^2(r_{01}) \equiv \int \mathrm{d}x_{12}\ p_{\parallel}(x_{12}|r_{01})(x_{12} - c_{\parallel}(r_{01}))^2.$$

The dependence on t of these quantities should be kept in mind.

As expected from the definition of $p_{\perp}$, the value of $c_{\perp}(r_{01})$ must be zero. We discussed in [Dol98] the fact that in the heterogeneous limit there is no back-dragging effect, i.e. $c_{zz}(z_{01}) = c_{\parallel}(r_{01}) = 0$, whereas in the homogeneous case we have $\sigma_{zz,\parallel,\perp}(r_{01}) = \text{constant}$ and $c_{zz,\parallel}(r_{01}) = \text{constant}$.

As shown in [Dol98], $c_{zz}(z_{01})$—which, by the way, is equal to $c_{\parallel}(r_{01})$—can account for anomalous diffusion in the β-domain. To be precise, we made use of the fact that $c_{zz}(z_{01}) \approx -cz_{01}$, where $c = c(t)$ is a constant. If we additionally assume that $p_{zz}(\cdot|z_{01})$ is Gaussian with constant width $\sigma_{zz}(z_{01}) = \sigma$, straightforward integration yields a connection between $c(t)$ and the approximate logarithmic slope

$$\beta(t) \equiv \frac{\ln\langle r^2(2t)\rangle - \ln\langle r^2(t)\rangle}{\ln 2t - \ln t} \approx \frac{\mathrm{d}}{\mathrm{d}\ln t} \ln\langle r^2(t)\rangle$$

of the mean square displacement, namely,

$$\beta(t) \approx 1 + \frac{\ln(1 - c(t))}{\ln 2}. \tag{1}$$

This estimate becomes incorrect for longer times, because the back-dragging is not linear any more. Mainly, this is the case because the particles start to leave their cages, which results in a more complex behaviour. This may explain the deformation of $c_{zz}(z_{01})$ and $c_{\parallel}(r_{01})$, which now look more like the first part of a negative sine function. To account for this effect, we define an 'effective' slope of $c_{zz}(z_{01})$, namely,

$$c_{\mathrm{eff}}(t) \equiv -\left(\int \mathrm{d}z_{01}\ p(z_{01}) z_{01} c_{zz}(z_{01})\right) \Big/ \langle z_{01}^2 \rangle \tag{2}$$

where all quantities depend on t.

Using $c_{\rm eff}(t)$ instead of $c(t)$ as input for equation (1), the approximation for β becomes exact. With $\langle r^2(t)\rangle = 3\langle z_{01}^2\rangle = 3\langle z_{12}^2\rangle$, we find that

$$\langle z_{02}^2\rangle = \langle (z_{01}+z_{12})^2\rangle = 2(\langle z_{01}^2\rangle + \langle z_{01}z_{12}\rangle)$$
$$\Leftrightarrow \frac{\langle z_{02}^2\rangle}{\langle z_{01}^2\rangle} = 2\left(1+\frac{\langle z_{01}z_{12}\rangle}{\langle z_{01}^2\rangle}\right)$$
$$\Leftrightarrow \beta \equiv \frac{\ln\langle z_{02}^2\rangle - \ln\langle z_{01}^2\rangle}{\ln 2} = 1 + \frac{\ln(1+\langle z_{01}z_{12}\rangle/\langle z_{01}^2\rangle)}{\ln 2} = 1 + \frac{\ln(1-c_{\rm eff}(t))}{\ln 2}.$$

If we had a purely heterogeneous scenario, where the conditional probability for the second move only depended on the length of the first one, i.e. $p_{zz}(z_{12}|z_{01};t) = p_{zz}(z_{12}||z_{01}|;t)$, then we would have

$$\langle z_{01}^2\rangle c_{\rm eff}(t) = \int {\rm d}z_{01}\ {\rm d}z_{12}\ p_{zz}(z_{12}||z_{01}|)p(z_{01})z_{01}z_{12} = 0$$

because $p(z_{01})$ is an even function. Therefore, $c_{\rm eff}(t)$ can be regarded as an appropriate measure for homogeneous contributions, and in the linear case it reduces to the slope $c(t)$. Hence homogeneous contributions strongly influence the nature of the anomalous diffusion.

4. The non-Gaussian parameter

A way to approach the high-density features of the self-part of the van Hove correlation function is to analyse the non-Gaussian parameter

$$\alpha_2(t) \equiv \frac{3\langle r^4(t)\rangle}{5\langle r^2(t)\rangle^2} - 1.$$

It measures the deviation from Gaussian behaviour and consequently has to vanish for $t \to 0$, because the dynamics on the very microscopic scale is Brownian by definition.

The NGP has been calculated for other systems, e.g. Lennard-Jones liquids [Kob95] and soft discs [Hur96]. In every case, a maximum has been found in the β-region, which becomes more pronounced as the temperature becomes lower.

In figure 3(a) we see $\alpha_2(t)$ for $\phi = 56\%$ as a dashed curve. It clearly does not decay to zero, but assumes a value $\alpha_2(\infty) \approx 0.15$. However, we must be careful with the definition of α_2, because the polydispersity can cause a trivial non-Gaussianity, due to a size-dependent particle mobility. Therefore, we should calculate the NGP for every particle diameter separately, and take the mean value over the size distribution afterwards; that is,

$$\alpha_{2,\rm poly}(t) \equiv \langle \alpha_{2,R}(t)\rangle_R.$$

Figure 3(a) shows this quantity for comparison. Thus, at this density, $\alpha_{2,\rm poly}(\infty) = 0$. The other two curves show the NGP, averaged over the 15% largest and the 15% smallest particles, respectively. Differing in their maximum values by about 10%, they exhibit a time separation of their maxima by a factor of three. Kob and Andersen have found the same dependence for their binary Lennard-Jones mixture [Kob95].

In figure 3(b), we see $\alpha_{2,\rm poly}(t)$ for different volume fractions in a double-logarithmic plot. For small times, one perceives a linear ascent which corresponds to an exponent of approximately 0.3. Later on, $\alpha_{2,\rm poly}$ reaches its maximum value at a time t_{α_2} in the late β-region and then slowly decreases again. As we can see, the maximum value of $\alpha_{2,\rm poly}$ grows with the density, i.e. $\alpha_{2,\rm max} = 0.17, 0.24, 0.56, 2.33$ for $\phi = 0.50, 0.53, 0.56, 0.58$, respectively. This strong dependence indicates a tremendous change of the dynamics for densities $\phi > 0.56$.

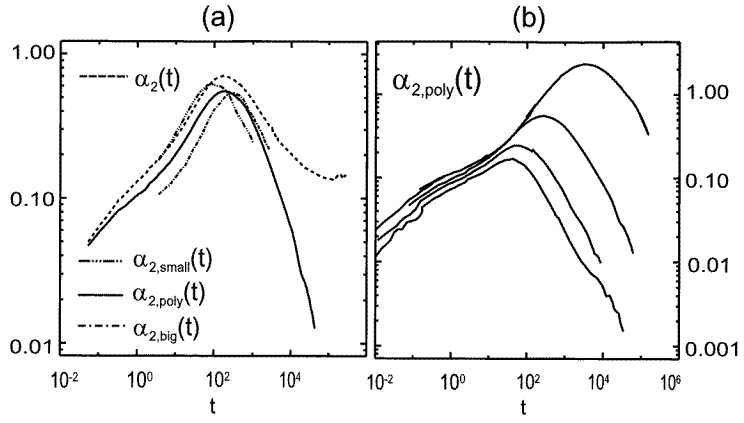

Figure 3. (a) The non-Gaussian parameter $\alpha_2 \equiv (3\langle r^4\rangle)/(5\langle r^2\rangle^2) - 1$ for density $\phi = 56\%$, calculated in different ways. For $\alpha_{2,\mathrm{small}}$, $\alpha_{2,\mathrm{big}}$ and α_2 the average is over the 15% smallest, the 15% biggest and all particles, respectively. For $\alpha_{2,\mathrm{poly}}$ the different sizes are treated separately, with the averaging performed afterwards, as discussed in the text. (b) The NGP $\alpha_{2,\mathrm{poly}}$ for the densities $\phi = 50$, 53, 56 and 58%, from bottom to top. Notice that the axes in (a) and (b) have been chosen to be logarithmic.

5. Three-time correlations: the heterogeneous part

It has been suggested that the value of $\alpha_2(t)$ is intimately connected with the existence of dynamic heterogeneities. For example, Hurley and Harrowell used a model of fluctuating mobilities to account for the non-Gaussian effects in a two-dimensional liquid [Hur96]. However, there are a few input parameters for this model, which must be adjusted to explain the simulation results, e.g. the functional form of the mobility autocorrelation. *A priori*, it is not clear to what extent the concept of fluctuating mobilities is reasonable, and a deeper understanding is still necessary to clarify the underlying physical mechanisms.

Again we analyse three-time correlations, now employing the information content of the widths $\sigma_{zz,\parallel,\perp}$. The important observation in figure 2 is that the length of the first step of a tagged particle has an influence on the mean size of its subsequent step, i.e. $\sigma_{zz}(z_{01})$ and $\sigma_{\parallel,\perp}(r_{01})$ grow with z_{01} and r_{01}, respectively. This can be understood in the following way. A fast particle in the first time interval on average remains fast during the second time interval, and so, by looking at $p_{zz}(\cdot|z_{01})$ or $p_{\parallel,\perp}(\cdot|r_{01})$ for large z_{01} or r_{01}, we select the most mobile particles. If we now calculate the degree to which σ_{zz} and $\sigma_{\parallel,\perp}$ grow with z_{01} and r_{01}, respectively, we have a direct measure of to what extent the dynamics is ruled by heterogeneities. For this purpose we define the quantity

$$a(t) \equiv \frac{\langle\sigma^4\rangle - \langle\sigma^2\rangle^2}{\langle\sigma^2\rangle^2} \tag{3}$$

where the brackets denote an average over the first step, i.e. $\langle\cdots\rangle \equiv \int \mathrm{d}r_{01}\cdots p(r_{01})$ or $\langle\cdots\rangle \equiv \int \mathrm{d}z_{01}\cdots p(z_{01})$. Here, a, σ and p have indices zz, $\parallel$ or $\perp$, depending on the probability function that is being analysed. (Note that a constant width σ results in a vanishing $a(t)$.)

Figure 4 shows $a_\parallel(t)$ and $a_\perp(t)$ for the density $\phi = 0.58$. We see that the broadening with r_{01} along the direction of the first step is greater than that perpendicular to it, resulting in a larger value of $a_\parallel(t)$. For longer times $t > \tau_\alpha$, however, the two curves coincide, indicating that there is no motional anisotropy with respect to the previous step any more. Collective flow

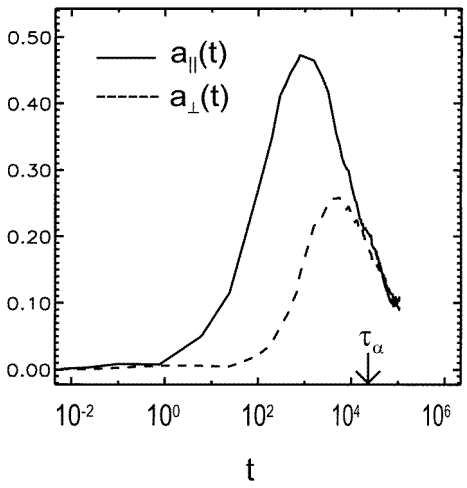

Figure 4. The quantities $a_{\|}(t)$ and $a_{\perp}(t)$, as defined in the text, for the density $\phi = 58\%$. The difference between the maximum values illustrates the fact that heterogeneities at intermediate times possess a directionality. For times greater than $\tau_\alpha \approx 2 \times 10^4$, the two curves meet each other, indicating the loss of anisotropy.

patterns, as observed for example by Donati *et al* [Don98], could cause such a directionality at intermediate times.

It is clear that $a(t) \neq 0$ should imply a non-vanishing NGP $\alpha_2(t)$. Figure 5 shows the relation between α_2 and the averaged $a_{3d}(t) \equiv (a_{\|} + 2a_{\perp})/3$. This surprising similarity of the time dependences of the two curves, suggests a deep physical connection. For a molecular

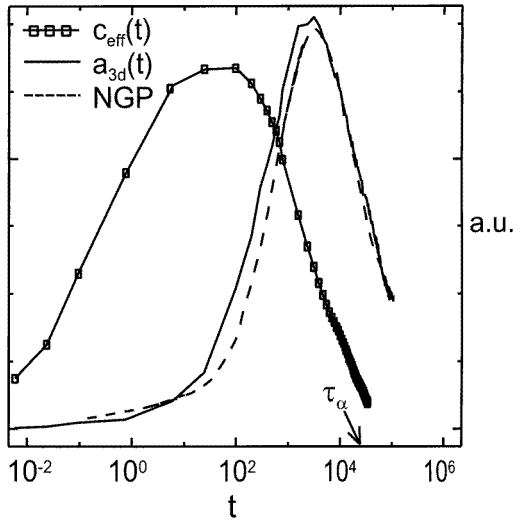

Figure 5. The averaged $a_{3d} \equiv (a_{\|} + 2a_{\perp})/3$, compared with the NGP α_2 and the effective slope $c_{\rm eff}(t)$ for density $\phi = 58\%$. a_{3d} and α_2 show the same behaviour with time, their maxima falling into the late β-region. $c_{\rm eff}(t)$, in contrast, is large only for times $t < \tau_\alpha$. Note that the units are arbitrary.

liquid, a similar observation has already been reported by Qian *et al* [Qia98], using another quantity similar to $a_{3d}(t)$. $c_{\mathrm{eff}}(t)$ is shown to allow a comparison of dynamical time regimes, reflecting the homogeneous contributions to the complex relaxation process.

6. Discussion

As a major result of this work we were able to quantify the homogeneous and the heterogeneous contributions to the non-exponential relaxation. We found that the anomalous diffusion is mainly related to homogeneous contributions, explicitly expressed by equations (1) and (2), whereas the non-Gaussian effects, displaying a maximum for the crossover between β- and α-relaxation, are mainly related to the heterogeneous contributions. This directly shows that, for the system studied in this work, the non-Gaussian effects, if present at all, are only mildly related to jump contributions. The maximum value of α_2 is of the same order as for the case of Lennard-Jones systems [Kob95]. There remains the interesting question of whether also for the Lennard-Jones system α_2 is mainly determined by heterogeneous contributions.

Relating the anomalous diffusion to homogeneous contributions, as discussed above, is only valid for stationary processes. As outlined, e.g., in reference [Ric94], continuous-time random walks, which by definition are purely heterogeneous in nature, are also able to generate anomalous diffusion behaviour. This, however, explicitly requires non-stationary conditions.

We would like to mention that $a(t)$, defined in equation (3), only takes into account heterogeneous contributions, related to the r_{01}-dependence of $\sigma_{\parallel,\perp}(r_{01})$, and neglects contributions resulting from the r_{01}-dependence of $c_{\parallel}(r_{01})$. A simple model system with $\sigma_{\parallel,\perp}(r_{01}) = \text{constant}$ and $c_{\parallel}(r_{01}) \propto -r_{01}$ is an ensemble of diffusive particles in identical harmonic potentials [Dol98]. The dynamics is purely Gaussian, i.e. $\alpha_2 \equiv 0$. Here the heterogeneity is related to the fact that particles which, by chance, are far away from the centre of the potential will experience a strong back-dragging force and will hence on average move further in the near future. As discussed in [Heu97], this effect can be also observed for the Rouse model of polymer dynamics. Note that on a qualitative level this type of heterogeneity is distinct from the type expressed by the r_{01}-dependence of $\sigma_{\parallel,\perp}(r_{01})$ for which the different mobilities are related to different environments.

Acknowledgments

We gratefully acknowledge helpful discussions with S Büchner and H W Spiess.

References

[Böh98] Böhmer R, Chamberlin R V, Diezemann G, Geil B, Heuer A, Hinze G, Kuebler S C, Richert R, Schiener B, Sillescu H, Spiess H W, Tracht U and Wilhelm M 1998 *J. Non-Cryst. Solids* **235–237** 1
[Cic90] Cichocki B and Hinsen K 1990 *Physica* A **166** 473
[Dol98] Doliwa B and Heuer A 1998 *Phys. Rev. Lett.* **80** 4915
[Don98] Donati C, Douglas J F, Kob W, Plimpton S J, Poole P H and Glotzer S C 1998 *Phys. Rev. Lett.* **80** 2338
[Edi96] Ediger M D, Angell C A and Nagel S R 1996 *J. Phys. Chem.* **100** 13 200
[Fuc98] Fuchs M, Götze W and Mayr M R 1998 *Phys. Rev.* E **58** 3384
[Heu97] Heuer A and Okun K 1997 *J. Chem. Phys.* **106** 6176
[Hur96] Hurley M M and Harrowell P 1996 *J. Chem. Phys.* **105** 10 521
[Kob95] Kob W and Andersen H C 1995 *Phys. Rev.* E **51** 4626
[Meg91] van Megen W and Pusey P N 1991 *Phys. Rev.* A **43** 5429
[Qia98] Qian J, Hentschke R and Heuer A 1998 *J. Chem. Phys.* at press
[Ric94] Richert R and Blumen A (ed) 1994 *Relaxational Processes* (Berlin: Springer)